Preparation and Properties of Crosslinked Multiblock Sulfonated Poly(arylene ether sulfone) Membranes for Fuel Cell Applications

Xuan Zhang, Zhaoxia Hu, Sha Zhang, Shouwen Chen, Shanshan Chen, Jianmei Liu, Lianjun Wang

School of Environmental and Biological Engineering, Nanjing University of Science and Technology, Nanjing 210094, China

ABSTRACT: Novel multiblock poly(arylene ether sulfone)s were prepared by a two-pot method from a phenoxide-end-capped fully disulfonated poly(arylene ether sulfone) oligomer and a fluoride-end-capped nonsulfonated poly(arylene ether sulfone) oligomer with block length of 10 as the hydrophilic and hydrophobic moieties, respectively, and were subsequently used as starting materials to be treated with phosphorous pentoxide (P_2O_5) to get crosslinked membranes. The crosslinking reaction occurred between the sulfonic acid groups and activated *ortho*-hydrogen atoms to the ether linkage of the hydrophobic units in the presence of P_2O_5 during solution casting. The crosslinking ratio was simply controlled by the amount of P_2O_5, and the fundamental properties of the resulting crosslinked multiblock membranes were investigated in detail. The water uptake and solution uptake in methanol solutions decreased with increasing crosslinking ratio, but a comparable high proton conductivity was maintained in the uncrosslinked membranes. They exhibited isotropic swelling behavior and largely enhanced dimensional stability in water and methanol solutions, whereas the uncrosslinked one showed anisotropic swelling behavior. The oxidative stability of the crosslinked membranes was significantly enhanced by the formation of sulfonyl linkages. The high proton conductivities at 120°C and 50% relative humidity suggested promising applications in elevated temperatures. © 2011 Wiley Periodicals, Inc. J Appl Polym Sci 121: 1707–1716, 2011

Key words: block copolymers; crosslinking; polyelectrolytes; poly(ether sulfones); swelling

INTRODUCTION

Currently, much effort has been devoted to the development of nonfluorinated polymer electrolyte membranes (PEMs) with high performance and sustainability to replace perfluorosulfonic acid membranes (e.g., Nafion, DuPont), which serve as proton conductors and fuel separators between anodes and cathodes in the applications of polymer electrolyte membrane fuel cells (PEMFCs) or direct methanol fuel cells (DMFCs).[1,2] Generally, an ideal PEM should meet the requirements of good proton conduction and mechanical properties, high chemical and thermal stability, and long-term durability.[3,4] Sulfonated aromatic hydrocarbon membranes are considered to be quite attractive PEM candidates for extensive temperature options as they exhibit glass temperatures well above the supposed operation temperatures and excellent mechanical toughness, low fuel permeability, and environmental friendliness. In contrast, expensive perfluorinated PEMs exhibit restricted operation temperatures (<110°C) and quite poor tolerance toward methanol solutions.[5,6] To date, many kinds of sulfonated nonfluorinated polymers, such as sulfonated poly(ether ketone)s,[7–9] sulfonated polyimides,[10–12] sulfonated polybenzimidazoles,[13–15] sulfonated polyphenylenes,[16–18] and sulfonated poly(arylene ether sulfone)s (SPAES),[19] have been developed successfully. Among them, SPAESs have been considered promising candidates because of their excellent thermal and oxidative stability, good mechanical properties, and processability, and their properties and performances for PEM applications have been explored extensively.[20]

More recently, the experimental results and conclusions of several research groups have suggested

that block ionomers are better candidates for PEM applications than random ones, with inspiring results, including the formation of a hydrophilic–hydrophobic phase-separation morphology and enhanced proton conductivity at lower relative humidities (RHs).[21–25] For example, Ghassemi and McGrath[23] prepared the multiblock SPAES polymers derived from phenoxide-terminated fully disulfonated poly(arylene ether sulfone) (BPSH) and decafluorobiphenyl or hexafluorobenzene end-capped unsulfonated poly(arylene ether sulfone) (BPS); the resulting membranes exhibited a well-defined hydrophilic–hydrophobic phase-separation morphology and a high proton conductivity of 15 mS/cm at 30°C under 30% RH, which was almost two times larger than that of Nafion 112. Watanabe et al.[24] also reported block SPAES containing fluorenyl groups with improved proton conduction properties. However, these multiblock membranes also exhibited an increase in the water uptake (WU) and physical swelling compared with the corresponding random ones at the similar ion exchange capacity (IEC) levels. For the BPSH–BPS PEMs with block lengths of 10–15 and an IEC of about 1.60 mequiv/g, the WUs and dimensional change in the thickness direction (Δt_c) increased to 60–74% and 70–80%, respectively, whereas they changed by only 35 and 15%, respectively, for the random one with an IEC of 1.53 mequiv/g.[25] This caused a large increase in membrane swelling and undesirable mechanical deterioration for the block membranes and was unfavorable for further PEMFC and DMFC applications.

Crosslinking is an effective method for enhancing the mechanical properties and suppressing membrane swelling so to improve membrane durability. There are lots of successful reports of crosslinking treatment, including (1) direct crosslinking by the introduction of a multifunctional crosslinking reagent during the polymerization stage[26–30] and (2) the postcrosslinking of a polymer or prepared membranes with specialized functionalized groups or sulfonic acid groups.[31,32] In the case of the direct crosslinking method, IEC and crosslinking degree could be controlled simply by the adjustment of the amount of crosslinking reagent, but gel formation phenomenon could occur during polymerization. Although in the case of the postcrosslinking method, the use of the sulfonic acid group itself seemed to be a smart choice because it was difficult to find other activated crosslinking positions in the hydrocarbon polymer system. Recently, Fang and coworkers[28–30] reported a facile approach for the preparation of crosslinked sulfonated hydrocarbon polymers based on the reaction between the sulfonic acid groups and activated hydrogen atoms in the presence of phosphorous pentoxide (P_2O_5). The resulting membranes exhibited a fairly enhanced stability toward water and better oxidative stability in Fenton's reagent due to the emergence of a quantity of oxidative stable sulfonyl groups and maintained satisfactory proton conduction properties, although IEC was sacrificed to an extent, up to 10%.

In our previous study, we applied this method for a random SPAES system and got satisfactory results. However, those crosslinked membranes showed some lower proton conductivity at higher crosslinking degrees. In this study, we conducted the postcrosslinking treatment for a multiblock SPAES membrane with a block length of 10. We investigated the postcrosslinking effect on the membrane proton conductivity, swelling behavior in water, and/or methanol solutions, and we report their properties, including WU, solution uptake (SU), dimensional changes in water and/or methanol solutions, hydrolytic and oxidative stability, and proton conductivity.

EXPERIMENTAL

Materials

4,4′-Difluorodiphenyl sulfone (DFDPS; Shou & Fu Chemical Co., Ltd., Zhejiang, China) and biphenol (BP; Yanhua Chemical Co., Ltd., Henan, China) were purified by sublimation before use. 3,3′-Disulfo-4,4′-difluorodiphenyl sulfone sodium salt (SDFDPS) was synthesized from DFDPS and purified according to the literature.[33] P_2O_5 (Kelong Chemical Reagent Factory, Chengdu, China) and fuming sulfuric acid (50%) (Zhenxin Chemical Reagent Factory, Shanghai, China) were used as received. Toluene was dried over P_2O_5, distilled at 140°C, and stored over 4-Å molecular sieves before use. Dimethyl sulfoxide (DMSO) was purified by stirring overnight over calcium hydride, distilled in vacuo at 120°C, and stored over 4-Å molecular sieves before use. Potassium carbonate was dried in vacuo at 120°C before use. Other reagents were used as received.

Synthesis of the multiblock copolymers

The multiblock copolymers were synthesized by nucleophilic polymerization via a two-pot method, as described in Scheme 1. Scheme 1 shows a typical procedure of BP–SDFDPS/DFDPS (10/10), where the figures in the parentheses refer to the lengths of the hydrophilic/hydrophobic blocks.

Phenoxide-end-capped hydrophilic oligomer

To a completely dried three-necked flask equipped with a mechanical stirrer, a Dean–Stark trap, a condenser, and a nitrogen inlet/outlet, 2.240 g (4.87 mmol) of SDFDPS, 0.819 g (4.40 mmol) of BP, 0.699 g (5.06 mmol) of potassium carbonate, 12.2 mL
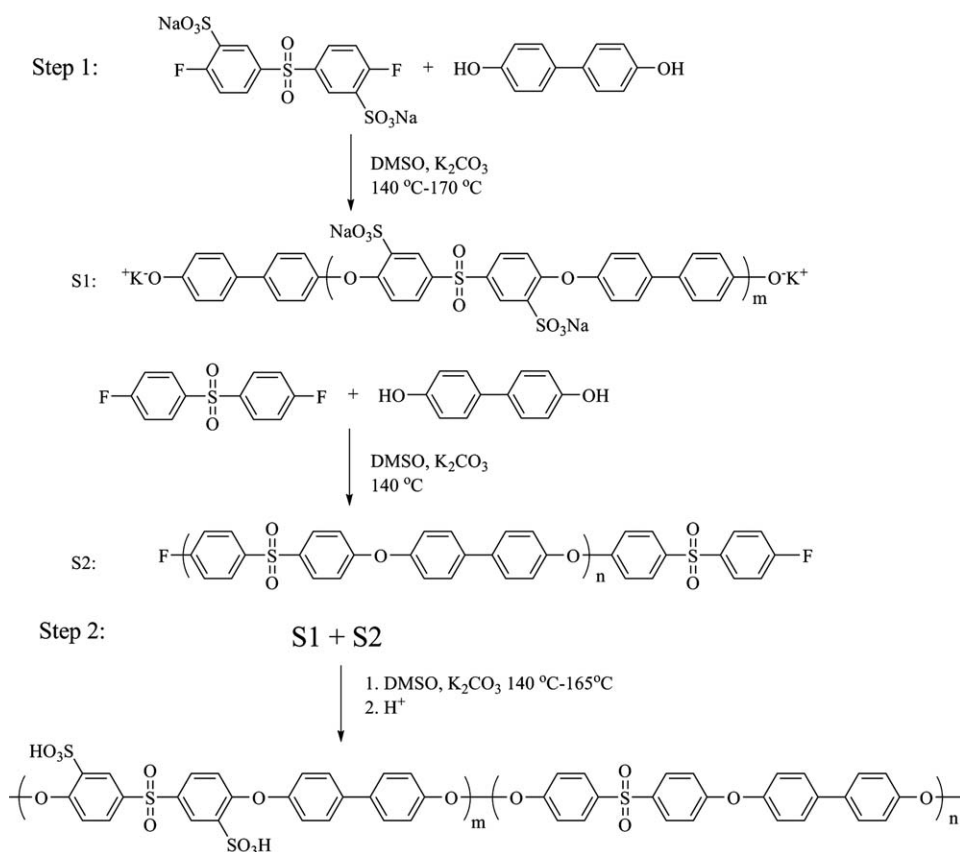
Scheme 1 Synthesis of the block SPAES. (S1 and S2 refer to the hydrophilic and hydrophobic oligomers, respectively.)

of DMSO, and 12.0 mL of toluene were charged. The mixture was allowed to reflux at 140°C for 4 h, and the produced water was removed with toluene as an azeotrope. Then, the reaction mixture was increased to 170°C for 2 h. The resulting product solution was cooled to room temperature for the next step.

Fluoride-end-capped hydrophobic oligomer

To another completely dried three-necked flask, which was equipped with a mechanical stirrer, a Dean–Stark trap, a condenser, and a nitrogen inlet/outlet, 1.243 g (4.87 mmol) of DFDPS, 1.001 g (5.34 mmol) of BP, 0.855 g (6.18 mmol) of potassium carbonate, 9.0 mL of DMSO, and 9.0 mL of toluene were charged. The mixture was allowed to reflux at 140°C for 2 h. Then, the resulting mixture was cooled to room temperature for the next step.

The hydrophobic oligomer solution was added carefully to the hydrophilic oligomer solution, and another 5.5 mL of toluene was added. The reaction mixture was increased to 140°C for 2 h to remove the produced water by toluene as an azeotrope. Then, the reaction mixture was slowly increased to 165°C, and the reaction proceeded for another 7 h. After it was cooled to room temperature, the resulting viscous solution was poured into water. The

resulting fiberlike precipitate was collected by filtration, acidified with 2M hydrochloric acid at 50°C for 72 h, then washed with water until it was neutral, and dried *in vacuo* at 80°C for 24 h. SPAES (4.810 g) in proton form was obtained, with a yield of 98%.

Crosslinking treatment

The crosslinking treatment was carried out by a dehydration reagent during a solution casting process. As an example, the experimental details for the crosslinking procedure are described as follows. A given amount of dry SPAES fiber (in proton form) and P_2O_5 were dissolved in DMSO at 30°C. The weight ratio of P_2O_5 to SPAES was controlled in the range 5–40%. The solution mixture was filtered, cast onto a glass plate, and dried at 80°C for 10 h at atmosphere. The glass plate was then moved to a vacuum oven and dried at 80°C for 1 h, 120°C for 2 h, and 170°C for 10 h successively. The resulting membrane was thoroughly rinsed with deionized water until it was neutral and then dried *in vacuo* at 120°C for 2 h and 150°C for 2 h.

Characterization

Fourier transform infrared (FTIR) spectra were recorded on a FTIR spectrometer (MB1545, Bomem, Canada) by

the attenuated total reflection (ATR) technique. The mechanical properties of the crosslinked membranes were analyzed by tensile measurement, which was performed with a universal testing instrument (AGS-X 349-05489A, Shimadzu, Japan) at 20°C and around 50% RH at a crosshead speed of 2 mm/min.

WU was measured according to a method described elsewhere.[34] The membranes were dried at 120°C *in vacuo* for 2 h to get the dry weight (W_d) and were then immersed in deionized water at given temperatures (30, 80, and 100°C) for 5 h. The swollen membrane was taken out, wiped with tissue paper quickly and weighed on a microbalance to obtain the wet weight (W_w). The WU of the membranes was calculated from eq. (1):

$$\text{WU}(\%) = (W_w - W_d)/W_d \times 100\% \qquad (1)$$

SU in methanol solutions was measured similarly to WU, where W_w' refers to the wet weight after immersion in the methanol solution. SU was calculated from eq. (2):

$$\text{SU}(\%) = (W_w\prime - W_d)/W_d \times 100\% \qquad (2)$$

IECs of the membranes were determined by a titration method. The proton-exchanged samples were first immersed in a 15 wt % NaCl solution for at least 72 h at 30°C, and then, the solutions were titrated with a 0.02M NaOH solution with phenolphthalein as the indicator. IEC was calculated from eq. (3):

$$\text{IEC} = C_{\text{NaOH}} \times V_{\text{NaOH}}/W_d \qquad (3)$$

where C_{NaOH} and V_{NaOH} are the concentration and volume of the NaOH solution, respectively.

We measured Δt_c and the dimensional change in the plane direction (Δl_c) by soaking two circular sample sheets in water or methanol solution at a given temperature for 5 h and calculated them from eq. (4):

$$\Delta t_c = (t - t_s)/t_s$$
$$\Delta l_c = (l - l_s)/l_s \qquad (4)$$

where t_s and l_s are the thickness and diameter, respectively, of the membrane equilibrated at 70% RH and t and l refer to the thickness and diameter, respectively, of the membrane immersed in water or a methanol solution.

The proton conductivity in the plane direction (σ) was determined with an electrochemical impedance spectroscopy technique over the frequency from 10 Hz to 100 KHz (Hioki 3532-50, Japan). A single cell with two platinum plate electrodes was mounted on a Teflon plate at a distance of 1.5 cm. The cells were placed in a thermocontrolled humidic vessel or in liquid water. σ was calculated from eq. (5):

$$\sigma = d/(\omega_s t_s R) \qquad (5)$$

where d is the distance between the two electrodes; t_s and ω_s are the thickness and width, respectively, of the membrane; and R is the resistance value measured. As for the measurements in liquid water, the swollen membrane thickness in water was used in the calculation of σ.

Water stability testing was carried out in water at 130°C for 24 h. The membrane toughness level was set as depicted elsewhere.[35] In level III, the membrane sheet breaks along a fold when it is folded to zero degree. In level IV, the membrane sheet breaks when it is folded back. In level V, the membrane sheet does not break after it is folded back.

We conducted oxidative stability testing by soaking a membrane sample (10 × 10 mm^2) in 50 mL of Fenton's reagent (30% H$_2$O$_2$ containing 30 ppm FeSO$_4$) at 30°C. We determined the stability by recording the time at which the film started to break into pieces and the time at which it eventually dissolved completely.

RESULTS AND DISCUSSION

In this study, the molar ratio of SDFDPS to DFDPS for both random (R-x membrane) and multiblock (B-x membrane) SPAES was 1 : 1, and in the multiblock polymer, the repeat units of the hydrophilic and hydrophobic blocks were 10, where x refers to the weight percentage ratio of P$_2$O$_5$ to SPAES.

Polymer synthesis, crosslinking, and characterization

The multiblock copolymer was synthesized by a two-pot method, as described in Scheme 1, which was similar to that reported by Watanabe et al.[36] In the first step, phenoxide-end-capped fully disulfonated hydrophilic oligomers and fluoride-end-capped unsulfonated hydrophobic oligomers were synthesized separately in the presence of potassium carbonate. In the second step, the oligomer solutions were mixed carefully and reacted at 165°C for 7 h to react adequately and to gain a high molecular weight. The instinct viscosity values of the resulting multiblock copolymer was 1.40 dL/g for a 0.5 wt % solution in DMSO at 35°C and 0.73 and 0.22 dL/g for the hydrophilic and hydrophobic oligomers, respectively. The high viscosity indicated a high molecular weight in the multiblock polymers.

As reported by Fang et al.,[29] a crosslinking reaction could be performed simply via the condensation between the sulfonic acid groups and the activated phenyl hydrogen atoms in the presence of the dehydration agent P$_2$O$_5$ and could result in very stable sulfonyl linkages. For the SPAES copolymers in this

TABLE I
Solubility of the Membranes Before and After the Crosslinking Treatment

	Solubility[b]				
Code[a]	DMSO	Dimethyl acetamide	N-methyl pyrrolidone	MeOH	EtOH
B-0	+	+	+	+−	−
B-5	+	+	+−	+−	−
B-10	−	−	−	−	−
B-20	−	−	−	−	−
B-40	−	−	−	−	−
R-0	+	+	+	+−	−
R-20	−	−	−	−	−

[a] B refers multiblock SPAES of BP–SDFDPS/DFDPS(10/10), and R refers random SPAES of BP–SDFDPS/DFDPS.
[b] +, soluble; −, insoluble on heating; +−, soluble on heating.

study, the *ortho*-hydrogen to the ether linkage in the BP moieties was available for the crosslinking reaction. In addition, they displayed good solubility in DMSO, meeting the condition proposed by Fang et al. By adjusting the weight ratio of P_2O_5 to dry polymer, we could easily control the crosslinking degree. For example, both the multiblock and random SPAES membranes exhibited similar IEC values by titration with the same crosslinking ratio (B-20 and R-20, as shown in Table I). During the solution casting process, a crosslinking reaction occurred between the sulfonic acid groups of the SDFDPS moieties and the activated hydrogen atoms of the BP moieties (Scheme 2). Figure 1 shows the possible configuration of the crosslinked membranes. We observed that all of the membranes became insoluble in organic solvents, including DMSO, after the crosslinking treatment, even at elevated temperatures, except those with a crosslinking ratio lower than 10%, as listed in Table I.

Figure 2 shows the FTIR-ATR spectra of the membranes before and after the crosslinking treatment. The intensity ratio calculated from the peak height ratio of the $O{=}S{=}O$ stretching vibrations of sulfonic acid groups at 1195 cm^{-1} (where no absorption band of sulfone group existed) to the peak at 1582 cm^{-1} assigned to aromatic $C{=}C$ stretching vibrations

decreased with increasing crosslinking ratio; that is, it was about 17% for the membrane of B-40 and 6% for B-10, which indicated that the crosslinking reaction was performed at the site of the sulfonic acid group.

Mechanical properties

Good physical strength and ductility are required in PEM fabrications for them to survive the stress of electrode attachment. Figure 3 shows the tensile stress–strain curves of the postcrosslinked membranes. The mechanical properties characterized were Young's modulus (M), maximum stress (S), and elongation at break (E_b). The data are listed in Table II. All of the crosslinked membranes displayed higher M, stress values, and lower elongation than the corresponding uncrosslinked one, with values of 1.65 GPa, 37.6 MPa, and 97.7%, respectively. This indicated that the crosslinked membranes obtained a much more compact structure because of the crosslinking method.

IEC, WU, and solvent uptake

Table III lists the IEC values by titration, WUs at 30–100°C, and corresponding hydration numbers (λs; the number of water molecules absorbed per sulfonic acid group) of the SPAES membranes. As shown in Table III, the titrated IEC values decreased from 2.04 to 1.43 as the crosslinking ratio increased from 0 to 40% due to the consumption of sulfonic acid groups.

In general, the crosslinked membranes displayed fairly lower WUs compared with the uncrosslinked ones because of their compact structure, as supposed previously. The WUs decreased with increasing crosslinking ratio, in accordance with their IECs. For example, at 30°C, the uncrosslinked membrane, B-0, showed a WU of 91%, whereas 70, 60, 52, and 35% WUs were observed for the B-5, B-10, B-20, and B-40 membranes, respectively. However, they still possessed better water-keeping capacities than their random references, such as the pair of B-20 and R-20, for the nature of block structure.

The influence of crosslinking on the methanol affinity was studied by evaluation of the membrane
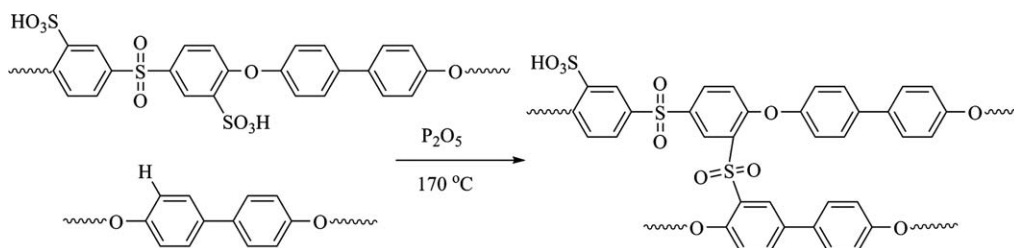
**Scheme 2** Crosslinking reaction of SPAES in the presence of P_2O_5.
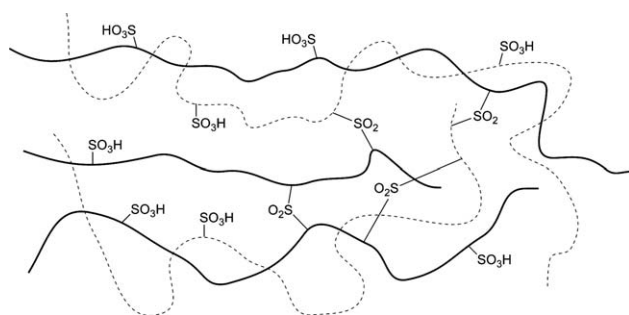
**Figure 1** Schematic diagram of the formation of cross-linked SPAES.

SU and swelling degree upon immersion in methanol solutions.[37] Generally, SU mainly depended on IEC, which was reported by the expanded framework of membranes opened by the absorbed water molecules, into which the methanol molecules could easily diffuse because of the hydrophilic properties of the sulfonate groups.[38] In this study, 30, 50, and 70% methanol solutions were chosen as the solutions. As shown in Figure 4, B-5 showed high SUs of 119, 195, and 250, which decreased to 75, 100, and 115 for B-20 in 30, 50, and 70% methanol solutions at 30°C, respectively. The SU values were much lower than those for the uncrosslinked one of 154, 287, and 438. They also exhibited rather lower SUs than Nafion 112; for example, B-40 exhibited an SU of 97 with 70% methanol solution at 60°C, which was almost half of that of Nafion 112; this suggested a lower methanol permeability in the crosslinked membranes.

Dimensional changes

Figure 5 shows the dimensional changes of the membranes in water. After the crosslinking treatment, all of the membranes displayed rather smaller
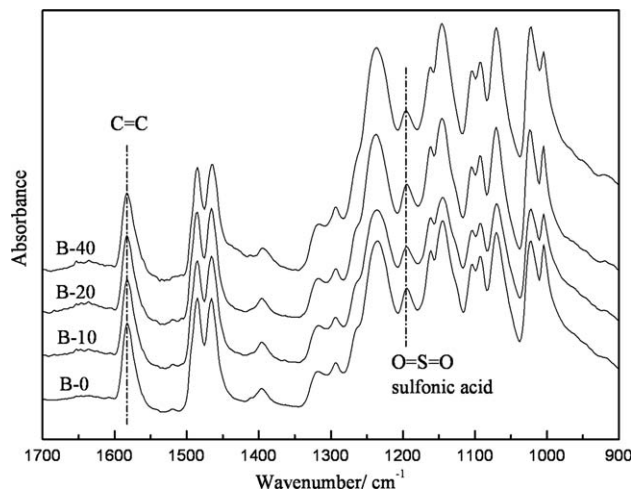
Figure 2 FTIR spectra of multiblock SPAES before and after the crosslinking treatment.
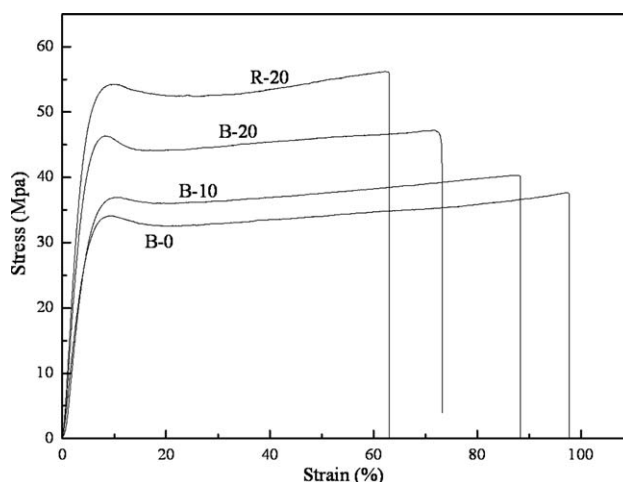
Figure 3 Tensile stress–strain curves of the crosslinked membranes.

Δt_c and Δl_c. For example, B-40 exhibited Δt_c and Δl_c values of 0.09 and 0.07, respectively, at 30°C and values of 0.12 in both the plane and thickness direction at 100°C; the values were 0.34 (Δt_c) and 0.21 (Δl_c) and 0.74 (Δt_c) and 0.50 (Δl_c) for the uncrosslinked B-0 at 30 and 100°C, respectively. The difference tended to be larger with increasing crosslinking ratio. For example, the dimensional changes of B-0 in both directions were four to five times that of B-40, about two times larger than those of B-20 at 30–100°C. At similar crosslinking ratios, such as B-20 and R-20, the multiblock membranes displayed slightly larger dimensional changes than the random ones; this might have been due to the more ordered hydrophilic clusters of the former from its block structure. The crosslinked membranes, especially at high crosslinking ratios, showed a larger Δt_c than Δl_c; this resulted in the conversion of distinct anisotropic dimensional changes of B-0 to the isotropic dimensional changes of the crosslinked membranes. The formation of rather stable sulfonyl linkages by crosslinking between the hydrophilic and hydrophobic segments of the polymer backbones enhanced the intermolecular interaction profoundly and, consequently, led to quite suppressed membrane swelling. It might be plausible that the sulfonyl groups produced during the crosslinking treatment acted as

TABLE II
Mechanical Properties of the Membranes

| Code | Stress–strain | | |
	M (GPa)	E_b (%)	S (MPa)
B-0	1.65	97.7	37.6
B-10	1.70	88.3	40.3
B-20	1.81	73.2	47.2
R-20	1.89	63.0	56.2

TABLE III
Physical Properties of the Membranes

Code	IEC[a]	WU (%)			λ			Proton conductivity (mS/cm)			
		30°C	80°C	100°C	30°C	80°C	100°C	50% RH[b]	70% RH[b]	In water[b]	50% RH[c]
B-0	2.04	91	157	293	25	43	80	18.6	57.8	322	211
B-5	1.95	70	98	196	20	28	56	16.9	51.1	287	187
B-10	1.86	60	86	170	18	26	51	14.4	46.4	251	162
B-20	1.80	52	67	137	16	21	42	13.1	41.3	220	142
B-40	1.43	35	43	55	14	17	21	8.3	23.4	97	90
R-0	1.95	86	116	212	25	33	60	13.8	39.0	179	146
R-20	1.77	46	61	108	14	19	34	10.6	26.2	99	96

[a] By titration.
[b] At 60°C.
[c] At 120°C.

bridges between the polymer chains and enhanced their interactions and made the intermolecular structure more compact; this led to the reduction of Δt_c. The isotropic membrane swelling behavior might have been evidence of the formation of a reticular structure inside the crosslinked multiblock membranes.

Table IV shows the dimensional changes of the crosslinked membranes in methanol solutions. As noted, the uncrosslinked B-0 exhibited rather poor dimensional stability. In 70% methanol solution, its Δt_c and Δl_c values were 0.88 and 1.02, respectively, at 30°C, and it was dramatically swollen and even lost mechanical properties when the temperature was increased to 60°C. On the other hand, the crosslinked membranes showed a highly enhanced dimensional stability in all of the methanol solutions. For example, B-20 showed Δl_c and Δt_c values of 0.28 and 0.33, respectively, in the 70% methanol solution at 30°C. B-40 displayed a Δt_c value of 0.15 and a Δl_c value of 0.10 in the 70% methanol solution at 30°C; these values just slightly increased to 0.20 and 0.11, respectively, at 60°C. This would be quite favorable

for DMFC performance because of the lower methanol permeation, as suggested by the reduced SU and swelling degree in methanol solutions.[37]

Water and oxidative stability

The water stability of the SPAES membranes was evaluated by accelerated aging tests at 130°C in water; this was followed by the investigation of the membrane toughness and weight loss. As shown in Table V, all of the crosslinked membranes displayed a toughness level of V after aging for 24 h and were tough enough to be bent or folded back without fracture. B-0 almost lost its mechanical properties and showed a weight loss over 8%, but B-20 and B-40 showed weight losses of only 2.7 and 0.5%, respectively. From the aspects of chemical structure, for the uncrosslinked multiblock membrane, its linear structure and enhanced hydrophilicity of the hydrophilic segment might have made it more susceptible to hydrolytic degradation than the crosslinked ones. This was reflected by the results of membrane toughness and weight loss.
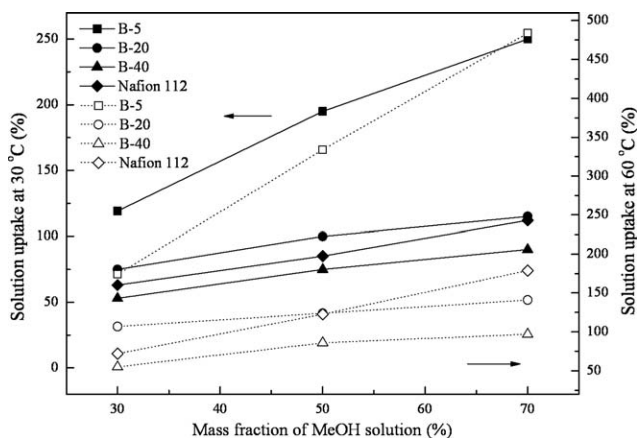

Figure 4 SU of membranes at different mass fractions of MeOH solution and temperatures (the closed and open symbols refer to membranes at 30 and 60°C, respectively).
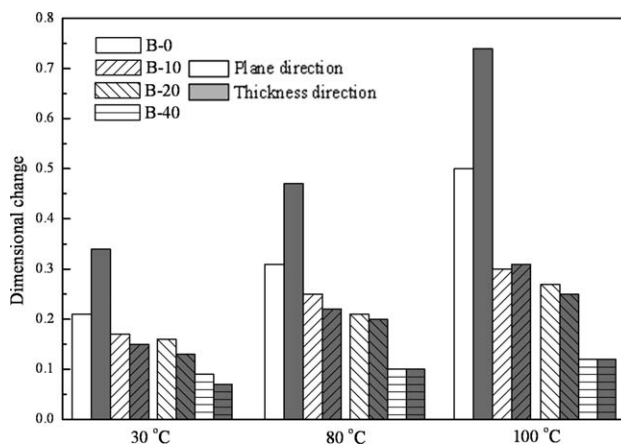

Figure 5 Dimensional changes of the membranes in water as a function of the temperature.

TABLE IV
Dimensional Changes of Membranes in Aqueous MeOH at Controlled Temperatures

	Dimensional change																			
	30°C												60°C							
	0%			30%			50%			70%			30%			50%			70%		
Code	Δl_c	Δt_c	ΔV^c	Δl_c	Δt_c	ΔV	Δl_c	Δt_c	ΔV	Δl_c	Δt_c	ΔV	Δl_c	Δt_c	ΔV	Δl_c	Δt_c	ΔV	Δl_c	Δt_c	ΔV
B-0	0.21	0.34	0.96	0.33	0.32	1.33	0.54	0.49	2.53	0.88	1.02	6.14	0.49	0.43	2.17	1.16	0.90	7.86	S[a]	S	–
B-5	0.19	0.16	0.64	0.28	0.32	1.16	0.41	0.44	1.86	0.60	0.65	3.22	0.39	0.44	1.78	0.58	0.68	3.19	0.81	0.88	5.16
B-10	0.17	0.15	0.57	0.22	0.26	0.88	0.29	0.28	1.13	0.37	0.38	1.59	0.26	0.28	1.03	0.35	0.39	1.53	0.45	0.46	2.07
B-20	0.16	0.13	0.52	0.20	0.16	0.67	0.25	0.28	1.00	0.28	0.33	1.18	0.23	0.25	0.89	0.28	0.31	1.15	0.31	0.36	1.33
B-40	0.09	0.07	0.27	0.04	0.09	0.18	0.08	0.11	0.29	0.10	0.15	0.39	0.08	0.12	0.31	0.09	0.14	0.35	0.11	0.20	0.48
R-0	0.13	0.23	0.57	0.30	0.29	1.18	–[b]	–	–	–	–	–	0.43	0.37	1.80	–	–	–	–	–	–
R-20	0.11	0.13	0.39	0.13	0.21	0.55	0.20	0.25	0.80	0.25	0.31	1.05	0.17	0.22	0.67	0.23	0.30	0.97	0.28	0.35	1.21

[a] Swollen.
[b] Not measured.
[c] Swelling rate in volume.

Figure 6 shows the weight residue of the membranes as a function of the soaking time in Fenton's reagent at 30°C. The uncrosslinked membrane B-0 almost started to lose weight at the beginning, and the membrane R-0 displayed a similar curve as B-0. Both of them were totally dissolved after 10 h. For the crosslinked membrane B-20, it had a weight residue of about 94%, and the mechanical strength was still maintained (not broken) after 11 h; this indicated a much enhanced oxidative stability.

It is well-known that the strong electron-withdrawing nature of sulfone (O=S=O) and pendent sulfonic acid groups will decrease the electron densities of nearby aromatic rings; thus, they could better tolerate electrophilic attack by hydroxyl radicals. Moreover, it could also be explained from the *ab initio* calculation proposed by Schuster et al.;[39] that is, electron-donating groups (—O—) in the ortho and para positions to the sulfonic acid group may have led to less hydrolytic stability. In this study, some sulfonic acid groups were converted to sulfone groups via crosslinking treatment, which lowered

the electron density of the polymer matrix and, hence, increased the oxidative stability.

Proton conductivity

Figure 7 shows σ as a function of RH at 60°C with those of Nafion 112 for comparison. Table II also lists the conductivity of the membranes at 50 and 70% RH in water at 60°C and at 50% RH at 120°C. All of the membranes exhibited comparable or even higher proton conductivities than Nafion 112 in water at 60°C; however, they showed a larger RH dependence than Nafion 112. With increasing crosslinking ratio, the proton conductivity decreased accordingly; this agreed with the general rule stating that the ionic conductivity of ion-exchange membranes is strongly related to their WU and IEC. For example, B-10, B-20, and B-40 showed σ values of 14.4, 13.1, and 8.3 mS/cm at 50% RH,

TABLE V
Water Stability of the SPAES Membranes

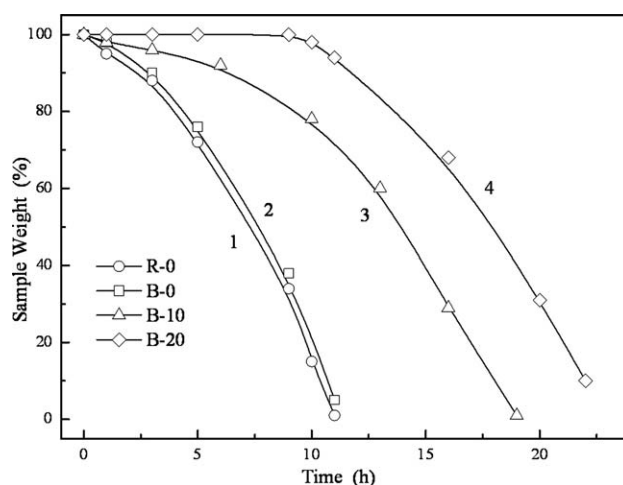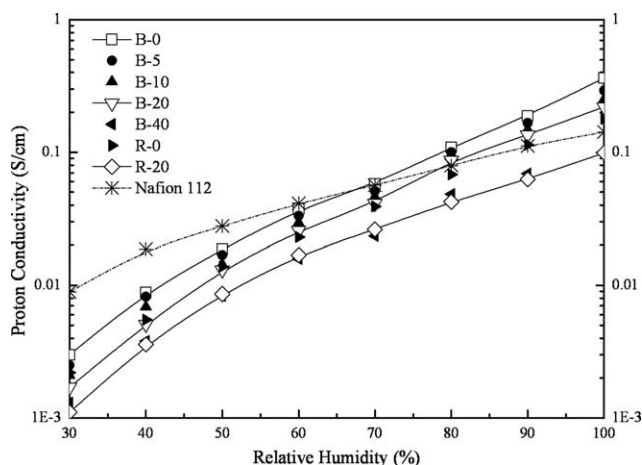|	Water stability[a]	
Code	Toughness	Weight loss (%)
B-0	III	8.4
B-5	V	7.8
B-10	V	5.5
B-20	V	2.7
B-40	V	0.5
R-0	V	8.0
R-20	V	2.3

[a] In water at 130°C for 24 h.
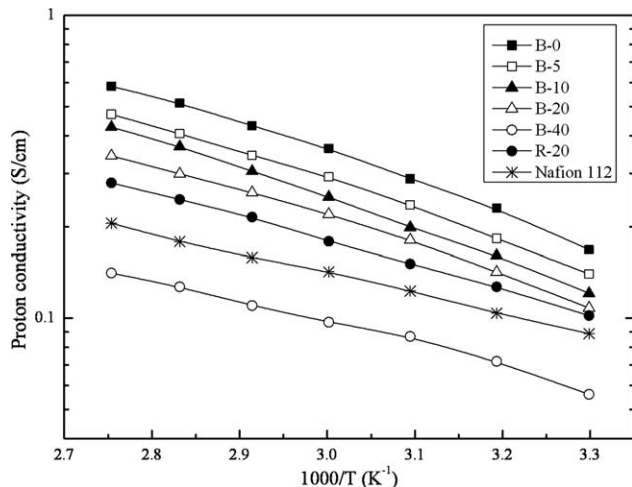

Figure 6 Oxidative aging of the membranes.

Figure 7 Proton conductivity of the crosslinked membranes and Nafion 112 as a function of the humidity at 60°C.

respectively, and B-0 showed a σ value of 18.6 mS/cm. With a similar crosslinking ratio, the B-20 membrane exhibited σ values almost 1.5 to 2 times as large as that of R-20 in the whole range. A possible explanation could be that although the crosslinking treatment might have disordered the cocontinuous hydrophilic domains in the multiblock membranes, most of them could still remain well enough to supply better proton transferring channels than those in the random ones. For the proton conductivity at 50% RH and 120°C, all of the membranes showed comparable or much higher values than the requirement (>0.1 S/cm) by the U.S. Department of Energy.[40]

Figure 8 shows the temperature dependence of the proton conductivity of the SPAES membranes and Nafion 112 in water. All of the σ values of the membranes were higher than that of Nafion 112 except

for that of B-40. The activation energy of the SPAES membranes was in the range 13–20 kJ/mol; this was a little larger than that of Nafion 112 (12 kJ/mol) and indicated their slightly weaker proton conductive capacity compared to Nafion 112.

CONCLUSIONS

A series of crosslinked multiblock SPAESs (block length = 10) was successfully prepared through dehydration reaction by the addition of P_2O_5, which converted sulfonic acid groups into stable sulfonyl linkages. Transparent and ductile membranes were obtained by solution casting. Their IEC, WU, and SU values decreased with increasing crosslinking ratio. The crosslinked multiblock membranes exhibited highly improved dimensional stability in water and methanol solutions, much enhanced stability toward water, and oxidative stability. They displayed a reasonably high proton conductivity; this indicated better comprehensive performance by the crosslinking method.

Figure 8 Temperature dependence of the proton conductivity of the SPAES membranes and Nafion 112 in water.

References

1. Mauritz, K. A.; Moore, R. B. Chem Rev 2004, 104, 4535.
2. Hickner, M. A.; Ghassemi, H.; Kim, Y. S.; Einsla, B. R.; McGrath, J. E. Chem Rev 2004, 104, 4587.
3. Li, Q.; He, R.; Jensen, J. O.; Bjerrum, N. J Chem Mater 2003, 15, 4896.
4. Kerres, J. J Membr Sci 2001, 185, 3.
5. Bae, J.-M.; Honma, I.; Murata, M.; Yamamoto, T.; Rikukawa, M.; Ogata, N. Solid State Ionics 2002, 147, 189.
6. Miyatake, K.; Chikashige, Y.; Higuchi, E.; Watanabe, M. J Am Chem Soc 2007, 129, 3879.
7. Jones, D. J.; Roziere, J. J Membr Sci 2001, 185, 41.
8. Kobayashi, T.; Rikukawa, M.; Sanui, K.; Ogata, N. Solid State Ionics 1998, 106, 219.
9. Liu, B.; Robertson, G. P.; Kim, D.-S.; Guiver, M. D.; Hu, W.; Jiang, Z. Macromolecules 2007, 40, 1934.
10. Fang, J.; Guo, X.; Harada, S.; Watari, T.; Tanaka, K.; Kita, H.; Okamoto, K. Macromolecules 2002, 35, 9022.
11. Hu, Z.; Yin, Y.; Chen, S.; Yamada, O.; Tanaka, K.; Kita, H.; Okamoto, K. J Polym Sci Part A: Polym Chem 2006, 44, 2862.
12. Chen, X.; Chen, K.; Chen, P.; Higa, M.; Okamoto, K.; Hirano, T. J Polym Sci Part A: Polym Chem 2010, 48, 905.
13. Li, Q. F.; Rudbeck, H. C.; Chromik, A.; Jensen, J. O.; Pan, C.; Steenberg, T.; Calverley, M.; Bjerrum, N. J.; Kerres, J. J Membr Sci 2010, 347, 260.
14. Jouanneau, J.; Mercier, R.; Gonon, L.; Gebel, G. Macromolecules 2007, 40, 983.
15. Li, Q.; Jensen, J. O.; Savinell, R. F.; Bjerrum, N. J. Prog Polym Sci 2009, 34, 449.
16. Fujimoto, C. H.; Hickner, M. A.; Cornelius, C. J.; Loy, D. A. Macromolecules 2005, 38, 5010.
17. Wu, S.; Qiu, Z.; Zhang, S.; Yang, X.; Yang, F.; Li, Z. Polymer 2006, 47, 6993.
18. Goto, K.; Rozhanskii, I.; Yamakawa, Y.; Otsuki, T.; Naito, Y. Polym J 2009, 41, 95.
19. Harrison, W. L.; Hickner, M. A.; Kim, Y. S.; McGrath, J. E. Fuel Cells 2005, 2, 201.

20. Wiles, K. B.; Wang, F.; McGrath, J. E. J Polym Sci Part A: Polym Chem 2005, 43, 2964.
21. Zhu, Z.; Walsby, N. M.; Colquhoun, H. M.; Thompsett, D.; Petrucco, E. Fuel Cells 2009, 4, 305.
22. Roy, A.; Lee, H.-S.; McGrath, J. E. Polymer 2008, 49, 5037.
23. Ghassemi, H.; McGrath, J. E. Polymer 2006, 47, 4132.
24. Bae, B.; Miyatake, K.; Watanabe, M. J Membr Sci 2008, 310, 110.
25. Lee, H.-S.; Roy, A.; Lane, O.; Dunn, S.; McGrath, J. E. Polymer 2008, 49, 715.
26. Mikhailenko, S. D.; Wang, K.; Kaliaguine, S.; Xing, P.; Robertson, G. P.; Guiver, M. D. J Membr Sci 2004, 233, 93.
27. Mikhailenko, S. D.; Robertson, G. P.; Guiver, M. D.; Kaliaguine, S. J Membr Sci 2006, 285, 306.
28. Fang, J.; Zhai, F.; Guo, X.; Xu, H.; Okamoto, K. J Mater Chem 2006, 17, 1102.
29. Zhang, G.; Guo, X.; Fang, J.; Chen, K.; Okamoto, K. J Membr Sci 2009, 326, 708.
30. Zhang, C.; Guo, X.; Fang, J.; Xu, H.; Yuan, M.; Chen, B. J Power Sources 2007, 170, 42.
31. Jorissen, L.; Gogel, V.; Kerres, J.; Garche, J. J Power Sources 2002, 105, 267.
32. Zhang, W.; Gogel, V.; Friedrich, K. A.; Kerres, J. J Power Sources 2006, 155, 3.
33. Bi, H.; Chen, S.; Gao, Z.; Zhang, S.; Wang, L. CIESC J 2009, 60, 2937.
34. Watari, T.; Fang, J.; Guo, X.; Tanaka, K.; Kita, H.; Okamoto, K. J Membr Sci 2004, 230, 111.
35. Yin, Y.; Suto, Y.; Sakabe, T.; Chen, S.; Hayashi, S.; Mishima, T.; Yamada, O.; Tanaka, K.; Kita, H.; Okamoto, K. Macromolecules 2006, 39, 1189.
36. Bae, B.; Miyatake, K.; Watanabe, M. Am Chem Soc Appl Mater Interfaces 2009, 1, 1279.
37. Bonis, C. de; D'Epifanio, A.; DiVona, M. L.; D'Ottavi, C.; Mecheri, B.; Tracersa, E.; Trombetta, M.; Licoccia, S. Fuel Cells 2009, 4, 387.
38. Bi, H.; Wang, J.; Chen, S.; Hu, Z.; Gao, Z.; Wang, L.; Okamoto, K. J Membr Sci 2010, 350, 109.
39. Schuster, M.; Kreuer, K.-D.; Andersen, H. T.; Maier, J. Macromolecules 2007, 40, 598.
40. U.S. Department of Energy. Hydrogen, Fuel Cells and Infrastructure Technologies Program, 2005–2015, 2011, http://www.nrel.gov/docs/fy05osti/34289.pdf